

# Continuous Adaptive Cross Approximation for Ill-posed Problems with Chebfun

A. Alqahtani · T. Mach · L. Reichel

February 7, 2022

**Abstract** The analysis of linear ill-posed problems often is carried out in function spaces using tools from functional analysis. However, the numerical solution of these problems typically is computed by first discretizing the problem and then applying tools from (finite-dimensional) linear algebra. The present paper explores the feasibility of applying the Chebfun package to solve ill-posed problems. This approach allows a user to work with functions instead of matrices. The solution process therefore is much closer to the analysis of ill-posed problems than standard linear algebra-based solution methods.

**Keywords** ill-posed problem, inverse problem, Chebfun, truncated SVE, Tikhonov regularization

**Mathematics Subject Classification (2010)** 47A52, 65F22, 45B05, 41A10

## 1 Introduction

We are interested in the solution of Fredholm integral equations of the first kind,

$$\int_{\Omega_1} \kappa(s, t)x(t) dt = g(s), \quad s \in \Omega_2, \quad (1.1)$$

---

Department of Mathematics, King Khalid University, P.O. Box 9004, Abha, Saudi Arabia and Department of Mathematical Sciences, Kent State University, Kent, OH 44242, USA. E-mail: aalqah11@gmail.com.

Department of Mathematical Sciences, Kent State University, Kent, OH 44242, USA. E-mail: thomas.mach@gmail.com.

Department of Mathematical Sciences, Kent State University, Kent, OH 44242, USA. E-mail: reichel@math.kent.edu.

---

with a square integrable kernel  $\kappa$ . The  $\Omega_i$  are subsets of  $\mathbb{R}^{d_i}$  for  $i = 1, 2$ . Such integral equations are common in numerous applications including remote sensing, computerized tomography, and image restoration.

Two major problems arise when solving (1.1). The first problem is that the space of functions is of infinite dimensionality. The second problem is that small changes in  $g$  may correspond to large changes in  $x$  as exemplified by

$$\max_{s \in \Omega_2} \left| \int_{\Omega_1} \kappa(s, t) \cos(2\pi mt) dt \right|, \quad \Omega_1 = \Omega_2 = [0, 1],$$

where the maximum can be made tiny by choosing  $m$  large, despite the maximum of  $|\cos(2\pi mt)|$  being 1. This is a consequence of the Riemann–Lebesgue theorem; see, e.g., [5, 7] or below for discussions of this result. The second problem is particularly relevant when the right-hand side  $g$  is a measured quantity subject to observational errors, as is the case in many applications.

Usually one deals with the first problem by first discretizing the functions  $x(t)$  and  $g(s)$  in (1.1) using  $n$  piecewise constant, linear, or polynomial basis functions; see e.g., [6] or [8]. The kernel  $\kappa(s, t)$  is discretized analogously. This transforms the problem into a system of linear equations. The second problem causes the coefficient matrix of said system to be ill-conditioned for sufficiently large  $n$ . Straightforward solution of these linear systems of equations generally is not meaningful because of severe error propagation. Therefore, this linear system has to be regularized. This can, for instance, be achieved by Tikhonov regularization or truncated singular value decomposition (TSVD). While the first dampens the influence of the small singular values, the latter outright ignores them. One is then often faced with a trade-off between a small discretization error and a small error caused by the regularization; see, e.g., Natterer [13]. In fact, often the more basis functions are used for the discretization, the more ill-conditioned the resulting coefficient matrix becomes, and the larger the need of regularization.

In this paper we will first regularize the problem and then discretize the problem. Regularization will be achieved through a singular value expansion of the kernel. At the same time the singular value expansion provides us with an excellent basis for discretizing the problem. The discretized problem is then a diagonal linear system of equations, which can be solved trivially. Thus, dealing with the second problem first simplifies the other problem.

We will compute the singular value expansion of the kernel using Chebfun [4]. Hence, our discretization basis will consist of piecewise Chebyshev polynomials. The computed solution is a Chebfun approximation to the function  $x(t)$ . The advantage of Chebfun is that the solution will feel and behave like a function. Therefore, our approach is arguably closer to directly solving (1.1) instead of a discretized version.

This paper is organized as follows. In the second section, we will provide basic definitions, introduce our notation, and briefly discuss Chebfun and singular value expansions. Section 3 discusses the truncated singular value expansion method (TSVE). The Tikhonov regularization method is described in Section 4. Numerical results that illustrates the performances of the methods

of Sections 3 and 4 are reported in Section 5. Concluding remarks can be found in Section 6.

## 2 Basics

Let  $L^2(\Omega_i)$  for  $i = 1, 2$  be spaces of Lebesgue measurable square integrable functions with inner products

$$\langle a(t), b(t) \rangle_{\Omega_i} = \int_{\Omega_i} \overline{a(t)} b(t) dt, \quad \text{for } i = 1, 2, \quad (2.1)$$

where  $\bar{a}$  represents the complex conjugate of  $a \in \mathbb{C}$ . Based on these inner products, we can define  $L^2$ -norms by

$$\|f(t)\|_{\Omega_i}^2 = \int_{\Omega_i} |f(t)|^2 dt, \quad \text{for } i = 1, 2.$$

Throughout this paper  $\|\cdot\|$  stands for an  $L^2$ -norm. We will omit the subscript if the domain is clear from the context. Since the spaces  $H_i := L^2(\Omega_i)$  for  $i \in \{1, 2\}$ , with the inner products and norms defined above, are complete vector spaces, they are *Hilbert space*; see, e.g., [6].

A given kernel  $\kappa(\cdot, \cdot) \in L^2(\Omega_1 \times \Omega_2)$  induces the bounded linear operator [6, Thm. 3.2.7]  $A : L^2(\Omega_1) \rightarrow L^2(\Omega_2)$  or  $H_1 \rightarrow H_2$  defined by

$$(Ax)(s) = \int_{\Omega_1} \kappa(s, t)x(t) dt. \quad (2.2)$$

The operator is sometimes called a *Hilbert-Schmidt integral operator* and the kernel  $\kappa$  a *Hilbert-Schmidt kernel*. This allows us to write (1.1) as

$$Ax = g. \quad (2.3)$$

In particular, we assume that  $g$  is in the range of  $A$ . Generally, we are interested in the solution of (2.3) of minimal norm. We refer to this solution as  $x_{\text{exact}}$ .

In practice, the right-hand side  $g$  of (1.1) is often a measured quantity and therefore is subject to observational errors. Thus, we assume that the error-free function  $g$  is not available—only an error contaminated approximation  $g^\delta \in H_2$  of  $g$  is known. We assume that  $g^\delta$  satisfies

$$\|g - g^\delta\| \leq \delta,$$

with a *known* bound  $\delta > 0$ . The solution of the equation

$$Ax = g^\delta, \quad \text{with } x \in H_1 \text{ and } g^\delta \in H_2, \quad (2.4)$$

is generally not a meaningful approximation of the desired solution  $x_{\text{exact}}$  of (2.3), since  $A$  is not continuously invertible. In fact, the equation (2.4) might not have a solution.

The operator  $A$  depends on the kernel  $\kappa$ . We will now have a closer look at known theory about the kernel function  $\kappa$ . For any square integrable kernel  $\kappa$ , we define the singular value expansion (SVE) [15, §4] as

$$\kappa(s, t) = \sum_i \sigma_i \phi_i(s) \psi_i(t). \quad (2.5)$$

The functions  $\phi_i(s)$  and  $\psi_i(t)$  are referred to as the singular functions. These functions are orthonormal with respect to the usual inner product (2.1) [15, §5], i.e.,

$$\langle \psi_i, \psi_j \rangle_{\Omega_1} = \langle \phi_i, \phi_j \rangle_{\Omega_2} = \delta_{ij}, \quad \text{with } i, j = 1, 2, \dots$$

The quantities  $\sigma_i$  are known as singular values. It can be shown that the only limit point of the singular values for square integrable kernels is zero [15, §5].<sup>1</sup> The singular values form a non-increasing sequence:

$$\sigma_1 \geq \sigma_2 \geq \sigma_3 \geq \dots \geq 0.$$

Let  $\sum_{i=1}^{\infty} \sigma_i \phi_i(s) \psi_i(t)$  be a uniformly convergent series. Then

$$\kappa(s, t) = \sum_{i=1}^{\infty} \sigma_i \phi_i(s) \psi_i(t), \quad (2.6)$$

as shown in [15, §8]. When the summation is finite, then the kernel  $\kappa(s, t)$  is said to be *separable* (or *degenerate*). Most applications do not have a separable kernel. However, if the kernel is square integrable, then it can be approximated well by a separable kernel with a suitable number of terms,  $\ell$ , in (2.6). Let

$$\kappa_{\ell} = \sum_{i=1}^{\ell} \sigma_i \phi_i(s) \psi_i(t), \quad (2.7)$$

with the same ordering of the singular values. Then this is the closest kernel of rank at most  $\ell$  to  $\kappa$  in the  $L^2$ -norm [15, §18 Approximation Theorem]. We will use this result to justify the application of the truncated singular value expansion method (TSVE), which will be discussed in Section 3.

We will also be using this Approximation Theorem to generally restrict our expansion to singular values greater than  $\varepsilon$ , where  $\varepsilon$  is a small enough cut-off—say  $10^{-8}$  or  $10^{-16}$ . Here, there is a trade-off between computing time and approximation accuracy. We try to choose  $\varepsilon$  far below the regularization error so that it does not have a significant effect on the accuracy. At the same time, a small  $\varepsilon$  means higher cost for computing the singular value expansion and forming the computed approximate solution.

In this paper we will use two regularization methods, TSVE and Tikhonov regularization. The TSVE method is based on the Approximation Theorem

<sup>1</sup>Schmidt calls the singular values eigenvalues, since he is mainly concerned with symmetric kernels and the concept of singular values was not developed when he published his paper. We follow modern notation here.

mentioned above. We approximate the kernel  $\kappa$  by  $\kappa_\ell$  for some suitable  $\ell \geq 0$ . This results in an approximation  $A_\ell$  to  $A$  and a solution, denoted by  $x_\ell$ , of the problem

$$(A_\ell x)(s) = \int_{\Omega_1} \kappa_\ell(s, t)x(t) dt = g^\delta(s), \quad s \in \Omega_2. \quad (2.8)$$

The parameter  $\ell$  is a regularization parameter that determines how many singular values and basis functions of  $\kappa$  are used to compute the approximate solution  $x_\ell$  of (2.4). The remaining singular values, which are smaller than or equal to  $\sigma_\ell$ , are ignored. The singular value  $\sigma_\ell$  provides information on the approximation error.

Tikhonov regularization replaces the system (2.4) by the penalized least-squares problem

$$\min_{x \in H_1} \{ \|Ax - g^\delta\|^2 + \lambda^2 \|x\|^2 \}, \quad (2.9)$$

which has a unique solution  $x_\lambda$  for any positive value of the regularization parameter  $\lambda$ . Substituting the SVE (2.5) into (2.9) shows that Tikhonov regularization dampens the contributions to  $x_\lambda$  of singular values and functions with large index  $k$  the most; increasing  $\lambda > 0$  results in more damping. Since we cannot deal with an infinite series expansion, we will, in practice, first cut-off all singular values that are less than  $\varepsilon$  as explained above, and then apply Tikhonov regularization.

The determination of suitable values of the regularization parameters,  $\ell$  in (2.8) and  $\lambda$  in (2.9), is important for the quality of the computed approximate solution. Several methods have been described in the literature including the discrepancy principle, the L-curve criterion, and generalized cross validation; see [3, 10, 11, 14] for recent discussions of their properties and illustrations of their performance. Regularization methods typically require that regularized solutions for several parameter values be computed and compared in order to determine a suitable value.

## 2.1 Chebfun

We solve (1.1) by first regularizing followed by discretization. However, we still want to compute the solution numerically. Thus, we need a numerical library that can handle functions in an efficient way. Since a function is representing uncountable many pairs of  $x$  and  $f(x)$  with  $x \mapsto f(x)$ , a computer can only handle approximations to functions numerically.<sup>2</sup>

We chose the Matlab package Chebfun [4] for this purpose. Chebfun uses piecewise Chebyshev polynomials, so called chebfuns, to approximate functions. All computations within Chebfun's framework are done with these approximations to the actual function. This in turn means that we project

<sup>2</sup>There are some notable exceptions like  $\sin(x)$  or  $x^2$ . However, we cannot assume that the solution of (1.1) will fall into this very small set of functions.

the functions  $g \in L^2(\Omega_2)$  onto a space of piecewise Chebyshev polynomials over  $\Omega_2$ . One can argue that this is a discretization. However, Chebfun's framework is significantly different from other discretizations in the sense that it gives the user the feeling of computing with functions.

Chebfun's functionality includes the computation of sums and products of functions and derivatives, inner products, norms, and integrals. Chebfun2/3, Chebfun's extension to functions of two and three variables, can also compute outer products and, most importantly for us here, the singular value expansion [16]. The algorithm behind the singular value expansion uses a continuous analogue of adaptive cross approximation. This is where some of the motivation for this work originates, since we recently analyzed the application of adaptive cross approximation to the solution of ill-posed problems [12].

The approximation of  $\kappa(s, t)$  is computed by an iterative process. First, an approximation of the maximum point  $(x, y)$  of  $\kappa(s, t)$  is determined. The computation of the exact maximum point is not important. The function is then approximated by

$$\kappa_1(s, t) = \frac{\kappa(s, y)\kappa(x, t)}{\kappa(s, t)},$$

where  $\kappa(s, y)$  and  $\kappa(x, t)$  are one-dimensional chebfuns in  $s$  and  $t$ , respectively.

This process is then repeated for  $\kappa(s, t) - \kappa_1(s, t)$  to find a rank-1 approximation of the remainder. By recursion one obtains after  $k$  steps a rank- $k$  approximation to the original kernel. As soon as the remainder is sufficiently small, the computed rank- $k$  approximation is the sought approximation to  $\kappa(s, t)$ . At the end we have  $\kappa(s, t) \approx C(s)DR(t)^T$ , with  $C(s)$  and  $R(t)$  vectors of functions, and  $D$  a dense matrix of size  $k \times k$ .

Based on this approximation it is easy to compute the singular value expansion. Chebfuns continuous analogue of the QR factorization can be used to find orthogonal bases for  $C(s)$  and  $R(t)$ . The upper triangular matrices are multiplied by  $D$  to form a new matrix  $\tilde{D}$ . Then a singular value decomposition of  $D = U\Sigma V^T$  is computed. Finally, the small orthogonal matrices  $U$  and  $V^T$  are combined with  $C(s)$  and  $R(t)$ , respectively; see [16]. A very similar process, called adaptive cross approximation [1, 2], was used in [12] for the discrete case of matrices and vectors.

Chebfun has some limitations. Currently only functions of at most three variables can be approximated by Chebfun. Hence, we are limited to ill-posed problems in one space-dimension, and to problems in two space-dimensions for which the kernel is separable and also given in a separable representation. This is the case for the kernel that models Gaussian blur in two space-dimensions, making Gaussian blur our only example in two space-dimensions in this paper.

Chebfun2 and Chebfun3 are further limited to domains that are tensor products of intervals. Thus, in this paper all domains are rectangles or rectangular boxes. Chebfun also needs multivariate functions to be of low rank for an efficient approximation, that is there has to exist a sufficiently accurate separable approximation. This is for instance not the case for the kernel  $\kappa(s, t) = st - \min(s, t)$  from the `deriv2` example of the Regularization Tools

package [8]. This limits the application of the methods described in this paper. However, the Chebfun package is still under development and some of the limitations mentioned might not apply to future releases.

### 3 The TSVE method

Assume that the kernel is non-separable and can be expressed as

$$\kappa(s, t) = \sum_{i=1}^{\infty} \sigma_i \phi_i(s) \psi_i(t), \quad (3.1)$$

and that the solution can be written as

$$x(t) = \sum_{j=1}^{\infty} \beta_j \psi_j(t). \quad (3.2)$$

The fact that  $\kappa$  is non-separable implies that all  $\sigma_i$  are positive, and the assumption that the solution is of the form (3.2) essentially states that the solution has no component in the null space of  $A$ . This assumption is justified since the null space of  $A$  is orthogonal to all the  $\psi_j$  and, thus, a component in the direction of the null space would increase the norm of the solution, but not help with the approximation of (1.1).

Substituting (3.1) and (3.2) into (1.1), and using the orthonormality of the basis functions yields

$$\sum_{i=1}^{\infty} \sigma_i \beta_i \phi_i(s) = g(s).$$

We further probe the equation with  $\phi_k(s)$  for all  $k$  and use the orthonormality of the basis functions to obtain

$$\sigma_k \beta_k = \int_{\Omega_2} \phi_k(s) g(s) ds, \quad \forall k.$$

Thus, the exact solution to (2.3) is given by

$$x(t) = \sum_{j=1}^{\infty} \beta_j \psi_j(t), \quad \text{with } \beta_j = \frac{\int_{\Omega_2} \phi_j(s) g(s) ds}{\sigma_j}. \quad (3.3)$$

If we truncate this series after  $\ell$  terms and use the noisy right hand side  $g^\delta$  instead of  $g$ , then we obtain the TSVE solution to (2.4) defined by

$$x_\ell(t) = \sum_{j=1}^{\ell} \beta_j^\delta \psi_j(t), \quad \text{with } \beta_j^\delta = \frac{\int_{\Omega_2} \phi_j(s) g^\delta(s) ds}{\sigma_j}. \quad (3.4)$$

The truncation parameter  $\ell$  can be chosen as needed.

In the following lemma, we link the projection of the error onto the space spanned by the  $\phi_i(s)$  to the norm of the error.

**Lemma 3.1** Let  $n(s) = g(s) - g^\delta(s)$  with  $\|n(s)\| \leq \delta$ . Then,

$$\sum_{i=1}^{\infty} \left( \int_{\Omega_2} \phi_i(s) n(s) ds \right)^2 \leq \delta^2, \quad (3.5)$$

where  $\phi_i(s)$  are orthonormal basis functions.

*Proof* Using the basis functions  $\phi_i(s)$ ,  $n(s)$  can be represented as

$$n(s) = \sum_{j=1}^{\infty} \gamma_j \phi_j(s) + \phi^\perp(s),$$

for certain coefficients  $\gamma_j$ , and where  $\phi^\perp(s)$  is orthogonal to all functions  $\phi_j(s)$ . Then,

$$\int_{\Omega_2} \phi_i(s) n(s) ds = \int_{\Omega_2} \phi_i(s) \left( \sum_{j=1}^{\infty} \gamma_j \phi_j(s) + \phi^\perp(s) \right) ds.$$

The orthogonality of the basis functions  $\phi_j$  allows us to simplify the above expression to

$$\int_{\Omega_2} \phi_i(s) n(s) ds = \gamma_i.$$

The same argument can be used to show that

$$\sum_{j=1}^{\infty} \gamma_j^2 \leq \|n(s)\|^2 \leq \delta^2.$$

Combining these results shows (3.5).  $\square$

We will now use the previous lemma to give an upper bound for the error of the solution obtained with the TSVE regularization method.

**Lemma 3.2** Let  $x(t)$  and  $x_\ell(t)$  be the exact solution and the TSVE regularized solutions given by (3.3) and (3.4), respectively. Assume the kernel  $\kappa(s, t)$  has finite rank  $r$ . Then,

$$\|x(t) - x_\ell(t)\| \leq \left( \frac{\delta^2}{\sigma_\ell^2} + \sum_{i=\ell+1}^r \beta_i^2 \right)^{1/2}. \quad (3.6)$$

*Proof* We will rely on the expansion of the solution in the space spanned by the functions  $\psi_i(t)$ . We have

$$\|x(t) - x_\ell(t)\|^2 = \left\| \sum_{i=1}^r \beta_i \psi_i(t) - \sum_{i=1}^{\ell} \beta_i^\delta \psi_i(t) \right\|^2.$$

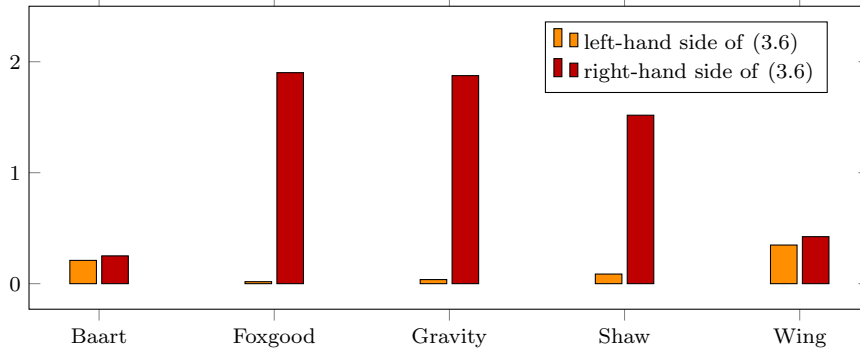


Fig. 3.1: Behavior of the bound (3.6) for the examples Baart, Foxgood, Gravity, Shaw, and Wing.

Using (3.3) and (3.4) this simplifies to

$$\begin{aligned} \|x(t) - x_\ell(t)\|^2 &= \left\| \sum_{i=1}^{\ell} \frac{\int_{\Omega_2} \phi_i(s)(g(s) - g^\delta(s)) ds}{\sigma_i} \psi_i(t) + \sum_{i=\ell+1}^r \beta_i \psi_i(t) \right\|^2 \\ &\leq \left\| \sum_{i=1}^{\ell} \frac{\int_{\Omega_2} \phi_i(s)(g(s) - g^\delta(s)) ds}{\sigma_i} \psi_i(t) \right\|^2 + \left\| \sum_{i=\ell+1}^r \beta_i \psi_i(t) \right\|^2. \end{aligned}$$

The orthonormality of the basis functions  $\psi_i$  allows us to simplify the above inequality to

$$\|x(t) - x_\ell(t)\|^2 \leq \sum_{i=1}^{\ell} \left( \frac{\int_{\Omega_2} \phi_i(s)(g(s) - g^\delta(s)) ds}{\sigma_i} \right)^2 + \sum_{i=\ell+1}^r \beta_i^2.$$

Using Lemma 3.5 and the fact the singular values are in non-increasing order gives

$$\|x(t) - x_\ell(t)\|^2 \leq \frac{\delta^2}{\sigma_\ell^2} + \sum_{i=\ell+1}^r \beta_i^2.$$

□

Lemma 3.2 provides a justification for choosing  $\ell$  such that

$$\sigma_\ell \leq \eta \delta,$$

with  $\eta$  being a small constant greater than 1. If  $\sigma_\ell = \delta$ , then the bound from Lemma 3.2 is at least 1. Choosing  $\eta$  larger means that  $\frac{\delta^2}{\sigma_\ell^2}$  will be smaller. However, there is a trade-off, since additional  $\beta_i$  have to be included in the

bound. Generally, choosing  $\eta$  between 2 and 5 is reasonable. Figure 3.1 illustrates the behavior of the bound (3.6) for some numerical examples.

Ill-posed problems based on one-dimensional integral equations are arguably less challenging than 2D-problems. Thus, consider the two-dimensional Fredholm integral equations of the first kind,

$$\int_{\Omega_1} \kappa(s_1, s_2, t_1, t_2)x(t_1, t_2) dt_1 dt_2 = g^\delta(s_1, s_2), \quad (s_1, s_2) \in \Omega_2. \quad (3.7)$$

We employ Chebfun for the numerical solution of the ill-posed problems. Hence, we are limited by Chebfun's capabilities to deal with higher-dimensional functions. A kernel that can be separated into a product of two functions, i.e.,  $\kappa(s_1, s_2, t_1, t_2) = \kappa_1(s_1, t_1) \times \kappa_2(s_2, t_2)$ , can be handled by Chebfun. The kernel that models Gaussian blur provides an example and will be used in a numerical illustration. Let the kernel be given by

$$\kappa(s_1, s_2, t_1, t_2) = \sum_{i=1}^{r_1} \sigma_i \phi_i^{(1)}(s_1) \psi_i^{(1)}(t_1) \sum_{j=1}^{r_2} \mu_j \phi_j^{(2)}(s_2) \psi_j^{(2)}(t_2), \quad (3.8)$$

where both the  $\sigma_i$  and  $\mu_j$  denote singular values, and let the solution be of the form

$$x(t_1, t_2) = \sum_{k=1}^{r_1} \sum_{\ell=1}^{r_2} \beta_{k\ell} \psi_k^{(1)}(t_1) \psi_\ell^{(2)}(t_2). \quad (3.9)$$

By substituting (3.8) and (3.9) into (3.7), and using the orthonormality of the basis functions, we get

$$\sigma_i \mu_j \beta_{ij} \phi_i^{(1)}(s_1) \phi_j^{(2)}(s_2) = g^\delta(s_1, s_2).$$

We further probe the equation with  $\phi_k^{(1)}(s_1) \phi_\ell^{(2)}(s_2)$  for all  $k$  and  $\ell$  and use the orthonormality of the basis functions to obtain

$$\beta_{ij} = \frac{\int_{\Omega_2} g^\delta(s_1, s_2) \phi_i^{(1)}(s_1) \phi_j^{(2)}(s_2) ds_1 ds_2}{\sigma_i \mu_j}. \quad (3.10)$$

This allows us to implement the solution algorithm using at most functions of three variables and, thus, not exceeding Chebfun3's capabilities [9].

In order to solve problems in two space-dimensions with a non-separable kernel, we would need Chebfun4, which currently is not available.

#### 4 Tikhonov regularization

For Tikhonov regularization, instead of solving (2.3) exactly, we solve the functional minimization problem

$$\min_{x \in H_1} \left\{ \|Ax - g^\delta\|^2 + \lambda^2 \|x\|^2 \right\}, \quad (4.1)$$

where  $\lambda$  is a fixed positive number. Using the definition of  $L^2$ -norm, equation (4.1) can be written as

$$\min_{x \in H_1} \left\{ \int_{\Omega_2} |Ax - g^\delta|^2 ds + \lambda^2 \int_{\Omega_1} |x|^2 dt \right\}. \quad (4.2)$$

By substituting (3.1) and (3.2) into (4.2), and by using the orthonormality of the basis functions, we obtain

$$\min_{x(t) \in H_1} \sum_{i=1}^{\infty} \left( \sigma_i^2 \beta_i^2 - 2\sigma_i \beta_i \int_{\Omega_2} \phi_i(s) g^\delta(s) ds + \lambda^2 \beta_i^2 \right) + \int_{\Omega_2} |g^\delta(s)|^2 ds.$$

Thus, we can compute the solution as

$$x_\lambda(t) = \sum_{j=1}^{\infty} \beta_j^{(\lambda)} \psi_j(t), \quad \text{with } \beta_j^{(\lambda)} = \frac{\sigma_j \int_{\Omega_2} \phi_j(s) g^\delta(s) ds}{(\sigma_j^2 + \lambda^2)}. \quad (4.3)$$

For the two-dimensional case, instead of solving (3.7) exactly, we solve

$$\min_{x(t_1, t_2) \in H_1} \left\{ \left\| \int_{\Omega_1} \kappa(s_1, s_2, t_1, t_2) x(t_1, t_2) dt_1 dt_2 - g^\delta(s_1, s_2) \right\|^2 + \lambda^2 \|x(t_1, t_2)\|^2 \right\}. \quad (4.4)$$

By substituting (3.8) and (3.9) into (4.4), and using the orthonormality of the basis functions, we get

$$\min_{x(t_1, t_2) \in H_1} \sum_{i=1}^{r_1} \sum_{j=1}^{r_2} \left( \beta_{ij}^2 \sigma_i^2 \mu_j^2 - 2\beta_{ij} \sigma_i \mu_j \int_{\Omega_2} \phi_i^{(1)}(s_1) \phi_j^{(2)}(s_2) g^\delta(s_1, s_2) ds_1 ds_2 + \lambda^2 \beta_{ij}^2 \right) + \int_{\Omega_2} |g^\delta(s_1, s_2)|^2 ds_1 ds_2, \quad (4.5)$$

and we can compute the solution by

$$x_\lambda(t_1, t_2) = \sum_{k=1}^{r_1} \sum_{\ell=1}^{r_2} \beta_{k\ell} \psi_k^{(1)}(t_1) \psi_\ell^{(2)}(t_2), \quad (4.6)$$

$$\text{with } \beta_{k\ell} = \frac{\sigma_k \mu_\ell \int_{\Omega_2} \phi_k^{(1)}(s_1) \phi_\ell^{(2)}(s_2) g^\delta(s_1, s_2) ds_1 ds_2}{\sigma_k^2 \mu_\ell^2 + \lambda^2}.$$

## 5 Numerical experiments

In this section we illustrate the performance of the methods described in Sections 3 and 4 by reporting some numerical results.

We first consider five test problems in one space-dimension. These problems are from Regularization Tools by Hansen [8]. This will be followed by applying the methods to a 2-D problem. All computations were carried out in MATLAB R2017a with about 15 significant decimal digits running on a laptop computer with core CPU Intel(R) Core(TM)i7-7Y75 @1.30GHz 1.60GHz processor with 16GB of RAM.

Each test problem from Regularization Tools by Hansen [8] provides us with an integral equation of the form (1.1). These problems are discretized by a Nyström method or a Galerkin method with orthogonal test and trial functions to give a linear system of equations  $\tilde{A}\mathbf{x} = \mathbf{g}$ , where  $\tilde{A} \in \mathbb{R}^{n \times n}$  is the discretized integral operator,  $\mathbf{x} \in \mathbb{R}^n$  is a discretization of the exact solution  $x_{\text{exact}}$ , and  $\mathbf{g} \in \mathbb{R}^n$  is the corresponding error-free right-hand side vector. We generate the error-contaminated vector  $\mathbf{g}^\delta \in \mathbb{R}^n$  according to

$$\mathbf{g}^\delta = \mathbf{g} + \alpha \frac{\|\mathbf{g}\|_2}{\|\mathbf{e}\|_2} \mathbf{e},$$

where  $\mathbf{e} \in \mathbb{R}^n$  is a random vector whose entries are from a normal distribution with mean zero and variance one. In our methods, we use the Matlab package Chebfun [4] to represent the kernel  $\kappa(s, t)$ , a function  $g(s)$  that represents the error-free right-hand side, and the desired solution  $x(t)$ . We define the error-contaminated function  $g^\delta(s)$  by

$$g^\delta(s) = g(s) + \alpha \frac{\|g(s)\|}{\|F(s)\|} F(s),$$

where  $F(s)$  is a smooth Chebfun function with maximum frequency about  $2\pi/\vartheta$  and standard normal distribution  $N(0, 1)$  at each point and  $\alpha$  is the noise level. In the computed examples, we let  $\vartheta = 10^{-2}$ . This is Chebfun's analogue to noise. Alternatively, we can use the discretized right-hand side from regularization tools [8].

The discrepancy principle is used to determine the truncation parameter  $\ell$  in (3.4) in the TSVE method, and the Tikhonov regularization parameter  $\lambda$  in (4.3). The discrepancy principle prescribes that the truncation index  $\ell$  be chosen as small as possible so that the solution  $x_\ell(t)$  of (3.4) satisfies

$$\left\| \int_{\Omega_1} \kappa(s, t) x_\ell(t) dt - g^\delta(s) \right\| \leq \eta \delta,$$

where  $\eta \geq 1$  is a user-supplied constant independent of  $\delta$ . The discrepancy principle, when used with Tikhonov regularization, prescribes that the regularization parameter  $\lambda > 0$  be chosen so that the solution  $x_\lambda$  of (4.1) satisfies

$$\left\| \int_{\Omega_1} \kappa(s, t) x_\lambda(t) dt - g^\delta(s) \right\| = \eta \delta.$$

We use the MATLAB function `fminbnd` to find the  $\lambda$ -value and we let  $\eta = 1$ .

One of the five test problems that we are interested in solving is Baart. This example is a Fredholm integral equation of the first kind (1.1) with  $\kappa(s, t) = \exp(s \cos(t))$ ,  $g(s) = 2 \sinh(s)/s$ , and solution  $x(t) = \sin(t)$ , where  $\Omega_1 = [0, \pi]$  and  $\Omega_2 = [0, \pi/2]$ .

We will compute approximate solutions of  $x(t) = \sin(t)$  by applying TSVE and Tikhonov regularization with Chebfun. These approximate solutions  $x_\ell(t)$  and  $x_\lambda(t)$  can be computed by using the formulas (3.4) and (4.3), respectively.

Fig. 5.1(a) displays the kernel  $\kappa(s, t)$  of the Baart example. The right-hand side function  $g(s)$  and the corresponding error-contaminated function  $g^\delta(s)$  are illustrated in Fig. 5.1(b), where the level noise is  $10^{-2}$ . Fig. 5.1(c) depicts the exact solution and the computed approximate solutions determined by TSVE and Tikhonov regularization with Chebfun. The latter figure shows that our methods give good approximation solutions of the exact solution.

Next, we will apply our methods to several different examples. Moreover, we will compare the methods with standard TSVD and Tikhonov regularization in discretized setting. The quality of the computed approximate solutions is measured with the relative error norm

$$RE := \frac{\|x_{\text{method}} - x\|_*}{\|x\|_*},$$

where  $\|\cdot\|_*$  denotes the Euclidean vector norm  $(\frac{1}{n} \sum_{i=1}^n x_i^2)^{1/2}$  if  $x$  is a vector, or the  $L^2$ -norm if  $x$  is a function.

Tables 5.1 and 5.2 compare the TSVE and Tikhonov regularization methods when used with Chebfun and with standard methods for the test problems Baart, Foxgood, Gravity, Shaw, and Wing from [8]. Three noise levels  $\alpha$  are considered. The number of discretization points,  $n$ , which is shown in the third column of the tables, is chosen to be between 1 and 2000, so that the smallest absolute difference between the relative error of the solution for the discretized problem and the relative error of the solution for the continuous problem is achieved. Thus, we choose the number of discretization points  $n$  so that the discretized problem gives an approximate solution of about the same accuracy as the approximate solution determined with Chebfun. This choice makes a comparison of the CPU-times required by the methods meaningful. The relative errors obtained by applying TSVD and Tikhonov regularization in the discretized setting are reported in the fourth column of Tables 5.1 and 5.2, respectively. The sixth column of the tables shows the relative errors obtained when applying TSVE and Tikhonov regularization with Chebfun. We also report the CPU times in seconds for each method in the fifth and seventh columns of tables. The tables show the computed approximate solutions determined by Chebfun-based methods to give as accurate approximations of the exact solutions as the approximate solutions determined by standard methods for the discretized problems. Moreover, we observe that the methods based on Chebfun are competitive time-wise for some problems, while they are slower for most problems. The last column of Tables 5.1 and 5.2 shows that applying TSVE with Chebfun is faster than applying Tikhonov regularization with

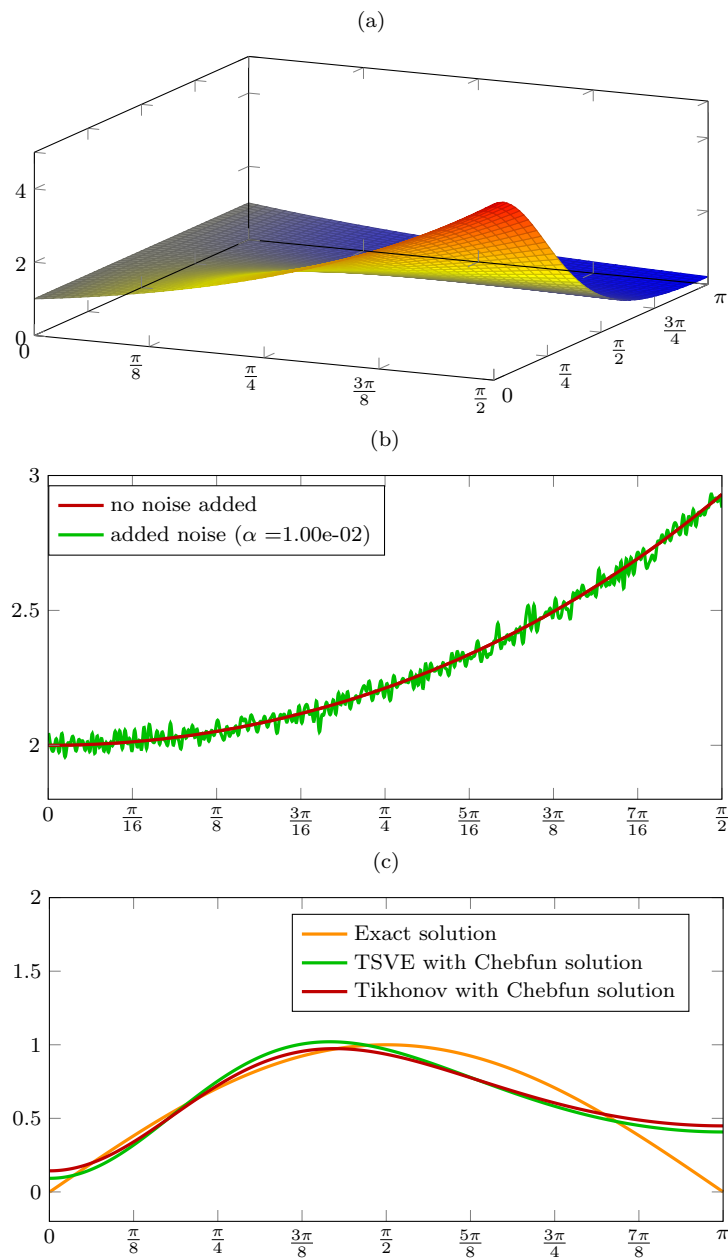


Fig. 5.1: Example –“Baart”: (a) Kernel , (b) Right-hand side, (c) Solutions.

Table 5.1: Comparison of TSVE with Chebfun and for the discretized problem.

Noise level	Example	n	discretized		with Chebfun	
			RE	CPU	RE	CPU
$10^{-3}$	baart	1376	$1.1479 \cdot 10^{-1}$	$2.1327 \cdot 10^0$	$1.1479 \cdot 10^{-1}$	$4.8078 \cdot 10^{-1}$
	foxgood	332	$9.8663 \cdot 10^{-3}$	$4.6138 \cdot 10^{-2}$	$9.8653 \cdot 10^{-3}$	$4.0253 \cdot 10^0$
	gravity	209	$1.9936 \cdot 10^{-2}$	$3.2203 \cdot 10^{-2}$	$1.9939 \cdot 10^{-2}$	$2.8642 \cdot 10^0$
	shaw	7	$3.9299 \cdot 10^{-2}$	$1.3183 \cdot 10^{-3}$	$4.1005 \cdot 10^{-2}$	$1.6327 \cdot 10^0$
	wing	822	$6.0280 \cdot 10^{-1}$	$2.9813 \cdot 10^{-1}$	$6.0280 \cdot 10^{-1}$	$5.2352 \cdot 10^{-1}$
$10^{-2}$	baart	470	$1.6644 \cdot 10^{-1}$	$7.6005 \cdot 10^{-2}$	$1.6644 \cdot 10^{-1}$	$1.6913 \cdot 10^{-1}$
	foxgood	327	$3.1572 \cdot 10^{-2}$	$2.5878 \cdot 10^{-2}$	$3.1575 \cdot 10^{-2}$	$1.8004 \cdot 10^0$
	gravity	152	$4.0750 \cdot 10^{-2}$	$4.6737 \cdot 10^{-3}$	$4.0751 \cdot 10^{-2}$	$1.0127 \cdot 10^0$
	shaw	720	$1.3119 \cdot 10^{-1}$	$2.4440 \cdot 10^{-1}$	$1.3087 \cdot 10^{-1}$	$1.0146 \cdot 10^0$
	wing	264	$6.0280 \cdot 10^{-1}$	$1.1490 \cdot 10^{-2}$	$6.0280 \cdot 10^{-1}$	$1.1596 \cdot 10^{-1}$
$10^{-1}$	baart	460	$3.4643 \cdot 10^{-1}$	$6.0992 \cdot 10^{-2}$	$3.4644 \cdot 10^{-1}$	$4.7546 \cdot 10^{-1}$
	foxgood	765	$7.5584 \cdot 10^{-2}$	$2.5744 \cdot 10^{-1}$	$7.5813 \cdot 10^{-2}$	$1.6939 \cdot 10^0$
	gravity	1730	$6.6598 \cdot 10^{-2}$	$3.6553 \cdot 10^0$	$6.6607 \cdot 10^{-2}$	$6.9005 \cdot 10^{-1}$
	shaw	1703	$1.5246 \cdot 10^{-1}$	$2.7470 \cdot 10^0$	$1.5267 \cdot 10^{-1}$	$4.2545 \cdot 10^{-1}$
	wing	276	$6.1568 \cdot 10^{-1}$	$2.2018 \cdot 10^{-2}$	$6.1542 \cdot 10^{-1}$	$5.0701 \cdot 10^{-1}$

Table 5.2: Comparison of Tikhonov regularization with Chebfun and for the discretized problem.

Noise level	Example	n	discretized		with Chebfun	
			RE	CPU	RE	CPU
$10^{-3}$	baart	184	$1.3228 \cdot 10^{-1}$	$6.9910 \cdot 10^{-3}$	$1.3220 \cdot 10^{-1}$	$2.8148 \cdot 10^0$
	foxgood	363	$1.2252 \cdot 10^{-2}$	$5.2424 \cdot 10^{-2}$	$1.2250 \cdot 10^{-2}$	$4.5776 \cdot 10^1$
	gravity	1250	$1.5306 \cdot 10^{-2}$	$1.1072 \cdot 10^0$	$1.5298 \cdot 10^{-2}$	$5.7426 \cdot 10^0$
	shaw	947	$4.4255 \cdot 10^{-2}$	$5.2421 \cdot 10^{-1}$	$4.4253 \cdot 10^{-2}$	$7.3928 \cdot 10^0$
	wing	1353	$6.0277 \cdot 10^{-1}$	$2.0925 \cdot 10^0$	$6.0277 \cdot 10^{-1}$	$1.0410 \cdot 10^1$
$10^{-2}$	baart	1332	$1.7066 \cdot 10^{-1}$	$1.6434 \cdot 10^0$	$1.7067 \cdot 10^{-1}$	$1.8585 \cdot 10^0$
	foxgood	1922	$2.3125 \cdot 10^{-2}$	$4.5407 \cdot 10^0$	$2.3124 \cdot 10^{-2}$	$3.7736 \cdot 10^1$
	gravity	1527	$2.8709 \cdot 10^{-2}$	$2.2178 \cdot 10^0$	$2.8708 \cdot 10^{-2}$	$5.3568 \cdot 10^0$
	shaw	186	$1.1000 \cdot 10^{-1}$	$1.5628 \cdot 10^{-2}$	$1.0998 \cdot 10^{-1}$	$5.5254 \cdot 10^0$
	wing	1232	$6.0340 \cdot 10^{-1}$	$1.4646 \cdot 10^0$	$6.0340 \cdot 10^{-1}$	$3.2663 \cdot 10^0$
$10^{-1}$	baart	568	$2.2781 \cdot 10^{-1}$	$1.3464 \cdot 10^{-1}$	$2.2769 \cdot 10^{-1}$	$1.7098 \cdot 10^0$
	foxgood	154	$5.4066 \cdot 10^{-2}$	$1.4565 \cdot 10^{-2}$	$5.4079 \cdot 10^{-2}$	$3.3878 \cdot 10^1$
	gravity	163	$8.8483 \cdot 10^{-2}$	$1.4838 \cdot 10^{-2}$	$8.8507 \cdot 10^{-2}$	$1.8138 \cdot 10^1$
	shaw	862	$1.6105 \cdot 10^{-1}$	$4.3403 \cdot 10^{-1}$	$1.6106 \cdot 10^{-1}$	$4.9331 \cdot 10^0$
	wing	12	$6.5959 \cdot 10^{-1}$	$6.1593 \cdot 10^{-3}$	$6.5836 \cdot 10^{-1}$	$7.2559 \cdot 10^0$

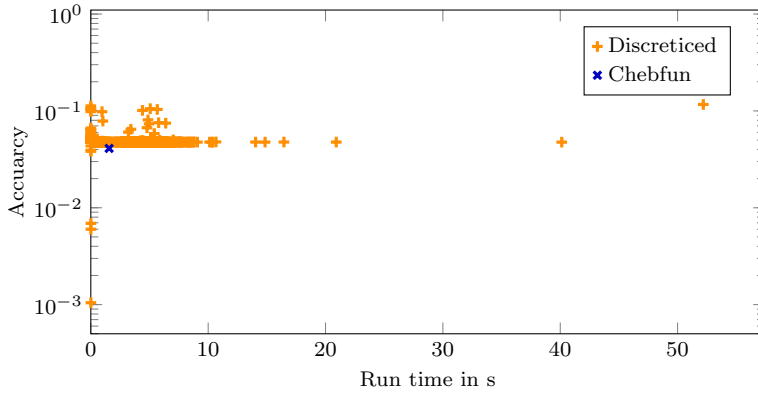


Fig. 5.2: Example—“Shaw”,  $\alpha = 1.00 \text{ e-}3$ .

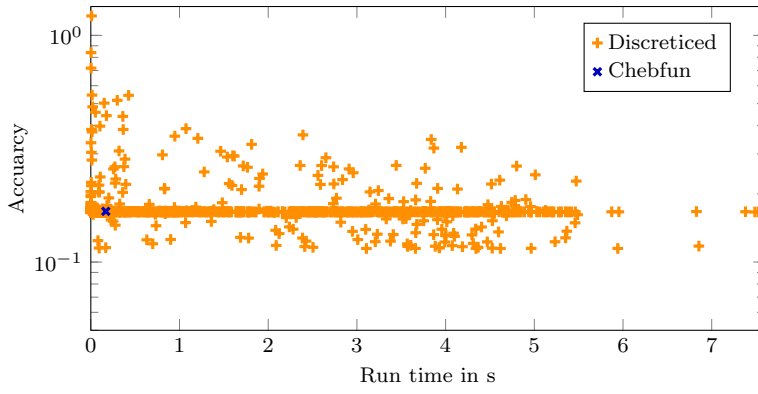


Fig. 5.3: Example –“Bart”,  $\alpha = 1.00 \text{ e-}2$ .

Chebfun. This is reasonable since the TSVE method does not require the use of a root-finder.

The accuracy and the run time for the discretized methods depend on the number of discretization points  $n$ ; Chebfun-based methods do not depend on  $n$ . Thus, in Figures 5.2, 5.4, and 5.4, we show some graphs with the relative accuracy on the vertical axis and run time on the horizontal axis; being closer to the origin is better. In the figures we trim some of the outliers when some values of  $n$  give bad accuracy. The figures show that the accuracy and computing time of the implementations with Chebfun are competitive.

Finally, we will consider a Fredholm integral equation of the first kind in two space-dimensions,

$$\int_{\Omega} \kappa(s_1, s_2, t_1, t_2)x(t_1, t_2) dt_1 dt_2 = g^{\delta}(s_1, s_2), \quad (s_1, s_2) \in \Omega, \quad (5.1)$$

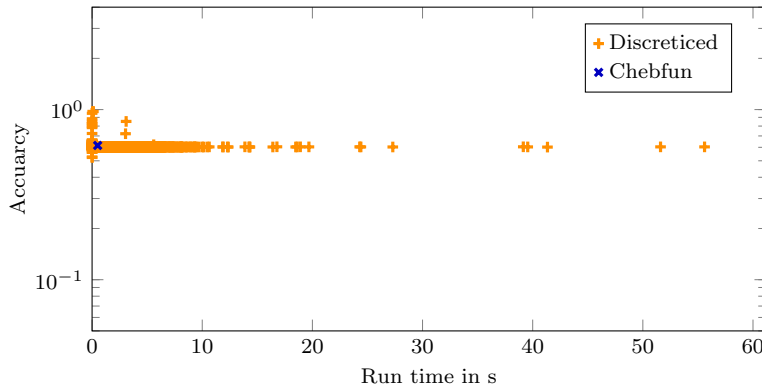


Fig. 5.4: Example –“Wing”,  $\alpha = 1.00 \text{ e} - 1$ .

where  $\Omega = [-1, 1] \times [-2, 2]$ . The kernel models Gaussian blur and is given by

$$\kappa(s_1, s_2, t_1, t_2) = \kappa_1(s_1, t_1) \times \kappa_1(s_2, t_2),$$

with

$$\kappa_1(s_1, t_1) = \frac{e^{-\frac{(t_1 - s_1)^2}{2\sigma^2}}}{\sqrt{2\pi\sigma^2}},$$

where  $\sigma$  is the standard deviation of the Gaussian distribution. The exact solution  $x(t_1, t_2)$  will be constructed as a continuous “image”<sup>3</sup> that we will blur and try to reconstruct. In our example, we let  $\sigma = 0.2$  and construct the exact solution as

$$x(t_1, t_2) = \{(t_1, t_2) \in \Omega : -0.5 < t_1 < 0.2 \text{ and } -0.6 < t_2 < -0.2\},$$

which is shown in Fig. 5.5(a). The error-free right-hand side function is determined by

$$g(s_1, s_2) := \int_{\Omega} \kappa(s_1, s_2, t_1, t_2) x(t_1, t_2) dt_1 dt_2$$

and the error-contaminated function  $g^\delta(s_1, s_2)$  in (5.1) is defined by

$$g^\delta(s_1, s_2) = g(s_1, s_2) + \alpha \frac{\|g(s_1, s_2)\|}{\|F(s_1, s_2)\|} F(s_1, s_2),$$

where  $F(s_1, s_2)$  is a smooth Chebfun function in two space-dimensions with maximum frequency about  $2\pi/\vartheta$  and standard normal distribution  $N(0, 1)$  at each point and  $\alpha$  is the noise level. In this problem, we let the noise level and  $\vartheta$  equal  $10^{-2}$ . Both the error-free right-hand side and the error-contaminated function are shown in Fig. 5.5(b) .

<sup>3</sup>With a continuous “image” we mean a mapping from  $[0, 1] \times [0, 1]$  to  $[0, 1]$ , where the function value represents a gray scale value. Thus, a gray scale value exists for all points continuously and not just for discrete points on a grid. The mapping itself is not necessarily continuous.

We reconstruct the exact image  $x(t_1, t_2)$  by applying the Chebfun-based methods to the problem. Similarly as for the problems in one space-dimension, the truncation parameter  $\ell$  in (3.9) and the Tikhonov regularization parameter  $\lambda$  in (4.6) are determined with aid of the discrepancy principle, where we set  $\eta$  to be 10 in our example. The reconstructed images obtained with the TSVE and Tikhonov regularization with Chebfun are shown in Fig. 5.5(c) and (d), respectively. The two reconstructed images are seen to be of roughly the same quality, with the image determined by Tikhonov regularization being slightly less oscillatory, and the computing times for both methods is comparable: the TSVE with Chebfun required 34.64 seconds, while Tikhonov regularization with Chebfun took 24.56 seconds.

## 6 Conclusion

The computed results illustrate the feasibility of using Chebfun to solve linear discrete ill-posed problems and in this way carry out computations in a fashion that is closer to the spirit of the analysis of ill-posed problems found, e.g., in [5]. The accuracy and timings of the implementations with Chebfun are competitive.

In the future further extensions to Chebfun including the treatment of functions of four or six variables will allow the application of the Chebfun-based approach discussed in this paper to the solution of linear ill-posed problems in two and three space-dimensions. It would be interesting to see if the observations made here carry over to these classes of problems.

## Acknowledgments

The authors are grateful for enlightening discussions with Behnam Hashemi (Shiraz University of Technology) about Chebfun and Chebfun3 in particular. We hope that this paper can serve as a motivation for the extension of Chebfun to four and higher dimensional functions.

We also would like to thank Richard Mikaël Slevinsky (University of Manitoba) for first pointing out to us the link between adaptive cross approximation and singular value expansions used in Chebfun2/3.

## References

1. M. BEBENDORF, *Approximation of boundary element matrices*, Numerische Mathematik, 86 (2000), pp. 565–589.
2. M. BEBENDORF AND S. RJASANOW, *Adaptive low-rank approximation of collocation matrices*, Computing, 70 (2003), pp. 1–24.
3. C. BREZINSKI, G. RODRIGUEZ, AND S. SEATZU, *Error estimates for linear systems with applications to regularization*, Numerical Algorithms, 49 (2008), pp. 85–104.
4. T. A. DRISCOLL, N. HALE, AND L. N. TREFETHEN, eds., *Chebfun Guide*, Oxford, 2014.
5. H. W. ENGL, M. HANKE, AND A. NEUBAUER, *Regularization of Inverse Problems*, Kluwer, Dordrecht, 2000.

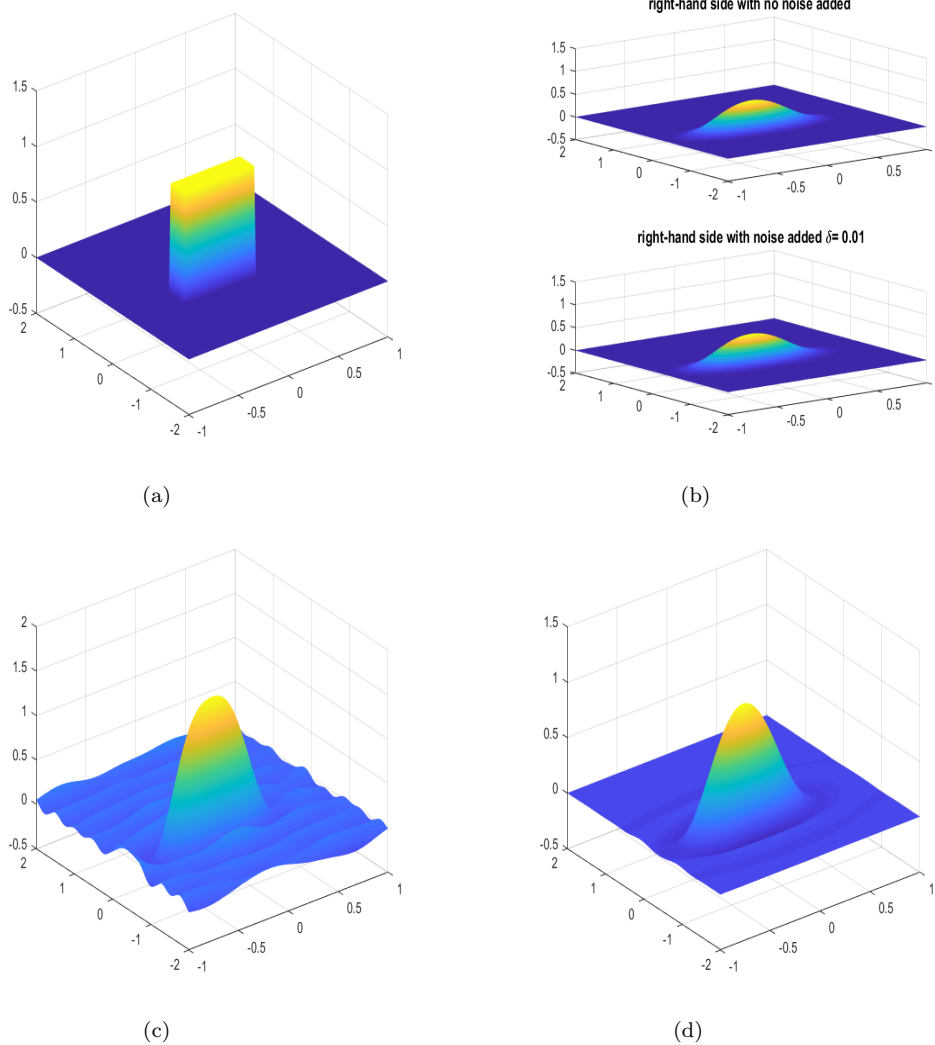


Fig. 5.5: Gaussian blur example: (a) Exact image, (b) Right hand side, (c) Reconstructed image by TSVE with Chebfun, (d) Reconstructed image by Tikhonov regularization with Chebfun.

6. W. HACKBUSCH, *Integral Equations: Theory and Numerical Treatment*, International Series on Numerical Mathematics, Birkhäuser, 1995.
7. P. C. HANSEN, *Rank-deficient and Discrete Ill-Posed Problems*, SIAM, Philadelphia, 1998.
8. P. C. HANSEN, *Regularization tools version 4.0 for Matlab 7.3*, Numerical Algorithms, 46 (2007), pp. 189–194.
9. B. HASHEMI AND L. N. TREFETHEN, *Chebfun in three dimensions*, SIAM Journal on Scientific Computing, 39 (2017), pp. C341–C363.

10. S. KINDERMANN, *Convergence analysis of minimization-based noise level-free parameter choice rules for linear ill-posed problems*, Electronic Transactions on Numerical Analysis, 38 (2011), pp. 233–257.
11. S. KINDERMANN AND K. RAIK, *A simplified L-curve method as error estimator*, Electronic Transactions on Numerical Analysis, 53 (2020), pp. 217–238.
12. T. MACH, L. REICHEL, M. VAN BAREL, AND R. VANDEBRIL, *Adaptive cross approximation for ill-posed problems*, Journal of Computational and Applied Mathematics, 303 (2016), pp. 206–217.
13. F. NATTERER, *Regularization of ill-posed problems by projection methods*, Numerische Mathematik, 28 (1977), pp. 329–341.
14. L. REICHEL AND G. RODRIGUEZ, *Old and new parameter choice rules for discrete ill-posed problems*, Numerical Algorithms, 63 (2013), pp. 65–87.
15. E. SCHMIDT, *Zur Theorie der linearen und nichtlinearen Integralgleichungen*, Vieweg+Teubner Verlag, Leipzig/Wiesbaden, 1989, pp. 190–233; reprint of an article from 1905.
16. A. TOWNSEND AND L. N. TREFETHEN, *An extension of Chebfun to two dimensions*, SIAM Journal on Scientific Computing, 35 (2013), pp. C495–C518.